

**GROWTH OF GaN FILMS ON GaAs (100)
SUBSTRATE BY RF-SPUTTERING AND E-BEAM
EVAPORATION TECHNIQUES**

MUHAMAD IKRAM BIN MD TAIB

UNIVERSITI SAINS MALAYSIA

2016

**GROWTH OF GaN FILMS ON GaAs (100)
SUBSTRATE BY RF-SPUTTERING AND E-BEAM
EVAPORATOR TECHNIQUES**

by

MUHAMAD IKRAM BIN MD TAIB

**Thesis submitted in fulfilment of the requirement for the degree of
Master of Science**

APRIL 2016

ACKNOWLEDGEMENT

In the name of Allah, the Entirely Merciful, the Especially Merciful.

My thanks are due in the first place to The Almighty, whose great mercy has allowed me to complete this dissertation successfully. I would like to extend my deepest gratitude to my supervisor, Dr. Norzaini Zainal, who has systematically guided and supported me throughout my period of research. Her soft approach and timely guidance enabled me to go through the project in a methodical manner. Without her help and support, I would have never been succeeded in achieving this milestone.

In the meantime, I also owe my deepest gratitude to my beloved colleagues, Esmed, Azharul, Alvin, Waheeda, Ezzah and Fatihah, who always helping and sharing their knowledge either theoretically or practically in order to ensure my research progress on schedule. Also not be forgotten my credit to Mrs. Rosfariza Radzali, who helping me in the porous experiment.

Besides, it gives me a great pleasure in acknowledging the support and help of NOR Lab staff, especially Mr. Anas Ahmad, Madam Ee Bee Choo, Mr. Jamil and Mr. Yushamdan. I also would like to thank Ministry of Education Malaysia for the MyBrain 15 scholarship programme that provides me with some financial support during my study. Last but not least, this thesis is dedicated to my beloved parents, ibu and ayah for their blessing and moral support. Not to be forgotten to my siblings for their support.

TABLE OF CONTENTS

	Page
ACKNOWLEDGEMENT	ii
TABLE OF CONTENTS	iii
LIST OF TABLES	vii
LIST OF FIGURES	viii
LIST OF SYMBOLS	xiv
LIST OF ABBREVIATIONS	xv
ABSTRAK	xix
ABSTRACT	xxi
CHAPTER 1: INTRODUCTION OF GaN SEMICONDUCTOR	1
CHAPTER 2: BASIC PROPERTIES AND LITERATURE REVIEW OF GaN	
2.1: Basic introduction to GaN material.....	6
2.2: Choice of substrate for GaN growth.....	9
2.2.1: Comparison between GaAs substrate and other substrate for GaN growth.....	10
2.2.2: GaAs surface orientation: GaAs (111) versus GaAs (100).....	11
2.3: Progress of GaN growth on foreign substrate.....	12
2.4: Role of buffer layer on growth of GaN material.....	20
2.5: Introduction of porous GaAs and its progress.....	24
2.6: Growth of GaN on porous GaAs/GaAs substrate.....	26
2.7: Post-annealing treatment as a way to improve GaN layer on GaAs substrate.....	27
2.8: Summary.....	28

CHAPTER 3: SAMPLE PREPARATIONS AND EXPERIMENTAL TECHNIQUES

3.1: Fabrication of porous GaAs/GaAs substrate.....	31
3.1.1: Optimizing electrolyte solution in fabrication of porous GaAs/GaAs substrate.....	33
3.1.2: Optimizing etching time in fabrication of porous GaAs/GaAs substrate.....	34
3.1.3: Optimizing DMF concentration in fabrication of porous GaAs/GaAs substrate.....	34
3.1.4: Optimizing current density in fabrication of porous GaAs substrate.	34
3.1.5: Optimizing applied voltage in fabrication of porous GaAs/GaAs substrate.....	34
3.1.6: Optimizing light sources in fabrication of porous GaAs/GaAs substrate.....	35
3.2: Growth of GaN layer on porous GaAs/GaAs substrate.....	35
3.2.1: Growth of AlN and TiN buffer layers.....	39
3.2.2: Growth of GaN layer by RF-sputtering.....	40
3.2.3: Growth of GaN layer by e-beam evaporation.....	41
3.3: Fabrication of porous GaN on GaN/GaAs substrate using electroless etching.....	43
3.4: Post-annealing treatment of GaN samples.....	45
3.5: Characterization measurements of GaN sample	47
3.5.1: Surface morphology analysis by FE-SEM measurement.....	48
3.5.2: Surface roughness analysis by AFM measurement.....	50
3.5.3: Structural studies by XRD measurement.....	52
3.5.4: Optical studies by PL measurement.....	55
3.5.5: Optical studies by Raman spectroscopy measurement.....	58
3.5.6: Elemental composition by XPS measurement.....	60

3.6: Summary.....	62
CHAPTER 4: FABRICATION OF HIGH QUALITY POROUS GaAs (100)	
4.1: Study of porous GaAs with different electrolyte.....	64
4.2: Study of porous GaAs with different etching time.....	71
4.3: Study of porous GaAs with different DMF concentration.....	72
4.4: Study of porous GaAs with different current density.....	76
4.5: Study of porous GaAs with different applied voltage.....	77
4.6: Study of porous GaAs with different light source.....	79
4.7: Summary.....	81
CHAPTER 5: STUDIES OF GALLIUM NITRIDE GROWN BY RF-SPUTTERING & ELECTRON BEAM EVAPORATION	
5.1: Growth of GaN layer using RF-sputtering.....	82
5.1.1: Preparation of nitride based buffer layers using RF-sputtering.....	84
5.1.2: Comparison of GaN layer grown on different surfaces.....	86
5.2: Growth of GaN layer using electron beam evaporation.....	91
5.3: Comparison between GaN layer grown by RF-sputtering and e-beam evaporation.....	95
5.4: Fabrication of porous GaN/GaN grown on GaAs substrate.....	98
5.4.1: Growth of thin GaN layer on GaAs substrate and with and without the insertion of AlN buffer layer.....	99
5.4.2: Porous GaN/GaN grown on GaAs substrate with and without the insertion of AlN buffer layer.....	104
5.5: Summary.....	110
CHAPTER 6: EFFECTS OF POST-ANNEALING TREATMENT OF GaN SAMPLES	
6.1: Post-annealing treatment of RF-sputtering GaN layer.....	111
6.2: Post-annealing treatment on GaN layer grown by electron beam evaporation.....	113

6.2.1: Effect of post-annealing temperature on the properties of GaN layer grown directly on GaAs by e-beam evaporation.....	113
6.2.2: Effect of post-annealing temperature on the properties of GaN layer grown on different surfaces.....	126
6.3: Summary.....	137
CHAPTER 7: CONCLUSIONS AND FUTURE WORKS.....	138
REFERENCES.....	142
LIST OF PUBLICATIONS.....	165

LIST OF TABLES

		Page
Table 2.1	Basic properties of hexagonal and cubic GaN structure.	9
Table 2.2	Summary of the GaN grown on foreign substrate with different buffer layer.	24
Table 3.1	Details of the types of electrolyte solution used to fabricate porous GaAs.	33
Table 3.2	Details of GaN layer grown on different type of surface using GaAs (100) substrate by RF-sputtering.	41
Table 3.3	Details of GaN layer grown on different surface of GaAs (100) substrate using electron beam evaporation.	43
Table 5.1	Differences between RF-sputtered and e-beam evaporated grown GaN layer on different surfaces.	96
Table 5.2	Details of the average pores size for porous GaN/GaN sample with and without the AlN buffer layer.	107
Table 6.1	Details of the annealed GaN layer grown on GaAs substrate by e-beam evaporation, at different annealing temperature.	114
Table 6.2	Details of the FWHM of the GaN (0002) orientation at different annealing temperature.	120
Table 6.3	Details of the FWHM and the intensity of NBE peak of the sample annealed at 950°C and 980°C.	122
Table 6.4	Details of the FWHM and peak shift of the GaN E ₂ (high) peak with different annealing temperature.	125
Table 6.5	Details of the annealed GaN layer grown on different surfaces at temperature of 980°C for 10 minutes under NH ₃ ambient by e-beam evaporation.	127
Table 6.6	Details of the FWHM, GaN E ₂ high peak position, GaN E ₂ (high) peak shifted and biaxial stress of the annealed GaN layer grown on GaAs substrate, nitride based buffer layers/GaAs substrate and porous GaAs/GaAs substrate at 980 °C for 10 minutes under NH ₃ ambient.	136

LIST OF FIGURES

		Page
Figure 2.1	Atomic arrangement in (a) hexagonal (wurtzite) and (b) cubic (zinc-blende) GaN material. The images were taken and modified from [5].	7
Figure 2.2	Stacking sequence of atoms in (a) hexagonal and (b) cubic structure. The images were taken and modified from [18].	8
Figure 2.3	Formation of mismatch dislocation in GaN layer grown directly on GaAs substrate. The image has been taken and modified from [90].	20
Figure 2.4	Schematic diagram to explain the idea of lattice arrangement in GaN layer grown on GaAs substrate (a) without and (b) with the insertion of buffer layer. The image is taken and modified from [91].	21
Figure 3.1	Flowchart of the research methodology in this work.	30
Figure 3.2	Schematic diagram of electrochemical etching experiment for fabricating porous GaAs from side view.	32
Figure 3.3	A modified schematic diagram of the working principle of RF-sputtering technique [136].	36
Figure 3.4	Schematic diagram of the RF-sputtering system at NOR Lab.	37
Figure 3.5	A modified schematic diagram of e-beam evaporation system [137].	38
Figure 3.6	Schematic diagram to describe the platinum (Pt) contact pattern on GaN/GaAs substrate by RF-sputtering.	44
Figure 3.7	A setup of the electroless etching technique of GaN sample.	45
Figure 3.8	Schematic diagram of 3-zone furnace for annealing treatment of GaN samples in this work.	47
Figure 3.9	A modified schematic diagram of FE-SEM system. Original image was taken from [139]	49
Figure 3.10	Schematic diagram of AFM system. The image was taken and modified from [140].	51
Figure 3.11	Calibration and tuning of (a) laser beam position and the total sum of the voltage and (b) the cantilever tuning in this work.	52

Figure 3.12	A modified schematic diagram of XRD operation in a crystal. This diagram was taken from [141].	53
Figure 3.13	Reported XRD data for GaN films (a) hexagonal GaN grown on GaAs (111) substrate [143] and (b) cubic GaN grown on GaAs (001) substrate [144].	55
Figure 3.14	Schematic diagram of PL system at 300K at the laboratory.	56
Figure 3.15	Schematic diagram of the beam dispersion in the monochromator. The diagram was modified from [145].	57
Figure 3.16	Schematic diagram of Raman spectra system at the laboratory.	59
Figure 3.17	The reported Raman spectrum of GaN layer using $z(x, \text{unpolarized})\bar{z}$ configuration [146]	60
Figure 3.18	Schematic diagram of the X-ray photoelectron process. This image has been modified from [147].	61
Figure 3.19	Reported data of XPS for GaN film grown on GaAs substrate [148].	62
Figure 4.1	Surface morphology of GaAs etched by $\text{H}_2\text{O}_2: \text{H}_3\text{PO}_4$ (5:1) at the magnification of (a) 1,000x, (b) 5,000x and (c) 10,000x, with current density, $J = 25 \text{ mA/cm}^2$ and time, $t = 10$ minutes.	65
Figure 4.2	Surface morphology of GaAs etched by 5% concentration of diluted NaOH at the magnifications of (a) 1,000x, (b) 5,000x and (c) 10,000x, with current density, $J = 25 \text{ mA/cm}^2$ and time, $t = 10$ minutes.	66
Figure 4.3	Surface morphology of GaAs etched by H_2SO_4 at the magnifications of (a) 1,000x, (b) 5,000x and (c) 10,000x, with current density, $J = 25 \text{ mA/cm}^2$ and time, $t = 5$ minutes.	67
Figure 4.4	Surface morphology of GaAs etched by HF: DMF (1:3) at the magnifications of (a) 1,000x, (b) 5,000x and (c) 10,000x, with current density, $J = 25 \text{ mA/cm}^2$ and time, $t = 10$ minutes.	68
Figure 4.5	Surface morphology of GaAs etched by HCl: DMF (1:3) at the magnification of (a) 1,000x, (b) 5,000x and (c) 10,000x, with current density, $J = 25 \text{ mA/cm}^2$ and time, $t = 10$ minutes.	69
Figure 4.6	Surface morphology of GaAs etched by HCl: DMF (1:3) at the magnification of (a) 1,000x (b) 5,000x and (c) 10,000x, with current density, $J = 25 \text{ mA/cm}^2$ and time, $t = 10$ minutes.	71

Figure 4.7	Surface morphology of GaAs etched with different etching time for (a) 10 minutes and (b) 20 minutes, at current density, $J = 25$ mA/cm ² in H ₂ SO ₄ : DMF (1:3).	72
Figure 4.8	Surface morphology of porous GaAs with the variation of DMF concentration in the mixture of H ₂ SO ₄ acid for (a) H ₂ SO ₄ : DMF (1:1), (b) H ₂ SO ₄ : DMF (1:3) and (c) H ₂ SO ₄ : DMF (1:9), at current density, $J = 250$ mA/cm ² and time, $t = 10$ minutes.	73
Figure 4.9	AFM images of 3D surface morphology of non-porous and porous GaAs with the variation of DMF concentration in the mixture of H ₂ SO ₄ acid for (a) non-porous, (b) H ₂ SO ₄ : DMF (1:1), (c) H ₂ SO ₄ : DMF (1:3) and (d) H ₂ SO ₄ : DMF (1:9), at current density, $J = 250$ mA/cm ² and time, $t = 10$ minutes.	75
Figure 4.10	FWHM versus DMF composition (in ratio) taken from (002) XRD rocking curve measurement.	76
Figure 4.11	Surface morphology of porous GaAs with variation of current density of (a) 25 mA/cm ² , (b) 250 mA/cm ² , (c) 350 mA/cm ² and (d) 250 mA/cm ² with improvement in current conductivity, at etching time, $t = 10$ minutes in the solution of H ₂ SO ₄ : DMF with the ratio of 1:3.	77
Figure 4.12	Surface morphology of GaAs etched with different voltage applied for (a) variation from 60 V, (b) 70 V and (c) 80 V, at time, $t = 10$ minutes using H ₂ SO ₄ : DMF solution with the ratio of 1:3.	78
Figure 4.13	Surface morphology of GaAs etched with different types of light source for (a) bulb, (b) UV lamp and (c) Xenon lamp, at current density, $J = \sim 250$ mA/cm ² and time, $t = 10$ minutes.	80
Figure 5.1	X-ray photoelectron spectroscopy (XPS) spectrum of GaN layer grown directly on GaAs substrate for (a) <i>Ga 3d</i> , (b) <i>N 1s</i> and (c) <i>O 1s</i> .	84
Figure 5.2	Surface morphology of nitride based buffer layer grown on GaAs (100) substrate of (a) AlN and (b) TiN.	84
Figure 5.3	3D-AFM image of nitride based buffer layer grown on GaAs (100) substrate for sample (a) Sample AB1 and (b) Sample TB1. The scan area was taken in (10 × 10) μm ² .	86
Figure 5.4	Surface morphology of the thick GaN grown on (a) GaAs substrate, (b) AlN buffer layer/GaAs substrate, (c) TiN buffer layer/GaAs substrate, (d) porous GaAs/GaAs substrate with the DMF concentration of 50% (e) 75% and (f) 90%. Inset figures show the surface morphology of the porous GaAs/GaAs substrate with different DMF concentration.	88

Figure 5.5	3D-AFM images of GaN layer grown on (a) GaAs substrate, (b) AlN buffer layer/GaAs substrate, (c) TiN buffer layer/GaAs substrate, (d) porous GaAs/GaAs substrate with the DMF concentration of 50%, (e) 75% and (f) 90% using RF-sputtering. The scan area was taken in $(10 \times 10) \mu\text{m}^2$.	90
Figure 5.6	Surface morphology of thick GaN layer grown on (a) GaAs substrate, (b) AlN buffer layer/GaAs substrate, (c) TiN buffer layer/GaAs substrate, (d) porous GaAs/GaAs substrate with the DMF concentration of 50%, (e) porous GaAs/GaAs substrate with the DMF concentration of 75% and (f) porous GaAs/GaAs substrate with the DMF concentration of 90%.	92
Figure 5.7	3D-AFM images of GaN layer grown by e-beam evaporation on (a) GaAs substrate, (b) AlN buffer layer/GaAs substrate, (c) TiN buffer layer/GaAs substrate, (d) porous GaAs/GaAs substrate with the DMF concentration of 50%, (e) 75% and (f) 90%. The scan area was taken in $(10 \times 10) \mu\text{m}^2$.	94
Figure 5.8	The surface roughness of the GaN layer grown by RF-sputtering and e-beam evaporation with respect to the different surface of GaAs.	97
Figure 5.9	Surface morphology of thin GaN grown on (a) GaAs substrate and (b) the AlN buffer layer/GaAs substrate.	100
Figure 5.10	3D-AFM image of the GaN layer grown on (a) GaAs substrate and (b) AlN buffer layer/GaAs substrate. The scan area was taken in $(10 \times 10) \mu\text{m}^2$.	101
Figure 5.11	X-ray diffraction (XRD) phase analysis scan of thin GaN layer directly grown on GaAs substrate.	102
Figure 5.12	Photoluminescence (PL) spectrum of the thin GaN layer directly grown on GaAs substrate and on AlN buffer layer/GaAs substrate.	103
Figure 5.13	Surface morphology of porous GaN/GaN fabricated using electroless etching technique with the AlN buffer layer at etching time (a) 3 minutes, (b) 5 minutes and without the AlN buffer layer at etching time (c) 3 minutes and (d) 5 minutes.	105
Figure 5.14	The proposed model of the etching mechanism during (a) 3 minutes of etching and (b) 5 minutes of etching. The 3 minutes etching gives more uniform in all directions and large pore than the 5 minutes etching. This model is applicable for GaN with and without the AlN buffer layer.	108

Figure 5.15	3D-AFM images of porous GaN/GaN fabricated using electroless etching with AlN buffer layer at etching time (a) 3 minutes, (b) 5 minutes and without AlN buffer layer at etching time (c) 3 minutes and (d) 5 minutes using $(10 \times 10) \mu\text{m}^2$ scanning area.	109
Figure 6.1	The image shows the condition of the RF-sputtering GaN sample grown on GaAs substrate, annealed at 700°C for 10 minutes under NH_3 ambient. Clearly, the GaN layer is peeled-off from the GaAs substrate.	112
Figure 6.2	Surface morphology of the annealed GaN layer grown directly on GaAs substrate by e-beam evaporation at different annealing temperature of (a) non-annealed, (b) 650°C , (c) 700°C , (d) 800°C , (e) 900°C , (f) 950°C , and (g) 980°C and (h) 1100°C , for 10 minutes under NH_3 ambient.	116
Figure 6.3	Dependence of the average surface roughness of the GaN layer grown directly on GaAs substrate by e-beam evaporation on annealing temperature, for 10 minutes under NH_3 ambient.	117
Figure 6.4	X-ray diffraction (XRD) phase analysis of the annealed GaN layer that directly grown on GaAs with different annealing temperature of (a) non-annealed, (b) 650°C , (c) 700°C , (d) 800°C , (e) 900°C , (f) 950°C , and (g) 980°C and (h) 1100°C , for 10 minutes under NH_3 ambient.	119
Figure 6.5	Photoluminescence (PL) spectra of the GaN layer grown directly on GaAs at different annealing temperature of (a) non-annealed (b) 650°C , (c) 700°C , (d) 800°C , (e) 900°C , (f) 950°C , (g), 980°C and (h) 1100°C , for 10 minutes under NH_3 ambient.	121
Figure 6.6	Raman spectra of the annealed GaN layer grown directly on GaAs with different annealing temperature of (a) non-annealed, (b) 650°C , (c) 700°C , (d) 800°C , (e) 900°C , (f) 950°C , (g) 980°C and (h) 1100°C , for 10 minutes under NH_3 ambient.	124
Figure 6.7	Surface morphology of the annealed GaN layer grown on (a) GaAs substrate, (b) AlN buffer layer/GaAs substrate, (c) TiN buffer layer/GaAs substrate, (d) porous GaAs/GaAs substrate with 50% DMF concentration, (e) porous GaAs/GaAs substrate with 75% DMF concentration and (f) porous GaAs/GaAs substrate with 90% DMF concentration, at 980°C for 10 minutes under NH_3 ambient.	128
Figure 6.8	3D-AFM images of the annealed GaN layer grown on (a) GaAs substrate, (b) AlN buffer layer/GaAs substrate, (c) TiN buffer layer/GaAs substrate, (d) porous GaAs/GaAs substrate with the DMF concentration of 50%, (e) 75% and (f) 90% by e-beam evaporation. The scan area was taken in $(10 \times 10) \mu\text{m}^2$.	130

- Figure 6.9 X-ray diffraction (XRD) phase analysis scan of the annealed GaN layer grown on (a) GaAs substrate, (b) AlN buffer layer/GaAs substrate, (c) TiN buffer layer/GaAs substrate, (d) porous GaAs/GaAs substrate with 50% DMF concentration, (e) porous GaAs/GaAs substrate with 75% DMF concentration and (f) porous GaAs/GaAs substrate with 90% DMF concentration, at 980°C for 10 min under NH₃ ambient. 132
- Figure 6.10 Photoluminescence (PL) spectra of the annealed GaN layer grown on (a) GaAs substrate, (b) AlN buffer layer/GaAs substrate, (c) TiN buffer layer/GaAs substrate, (d) porous GaAs/GaAs substrate with 50% DMF concentration, (e) porous GaAs/GaAs substrate with 75% DMF concentration and (f) porous GaAs/GaAs substrate with 90% DMF concentration, at 980°C for 10 min under NH₃ ambient. 133
- Figure 6.11 The FWHM of the NBE related emissions of the GaN layer grown by e-beam evaporation with respect to the different surface of GaAs. 134
- Figure 6.12 Raman spectra of the annealed GaN layer grown on (a) GaAs substrate, (b) AlN buffer layer/GaAs substrate, (c) TiN buffer layer/GaAs substrate, (d) porous GaAs/GaAs substrate with 50% DMF concentration, (e) porous GaAs/GaAs substrate with 75% DMF concentration and (f) porous GaAs/GaAs substrate with 90% DMF concentration, at 980°C for 10 min under NH₃ ambient. 135

LIST OF SYMBOLS

J	Current density
t	Time
E_g	Energy band gap
χ	Electron affinity
T	Temperature
m_e	Effective electron mass
a_o	Lattice constant along a -direction
c_o	Lattice constant along c -direction
λ	Wavelength
σ	Biaxial stress

LIST OF ABBREVIATIONS

AlN	Aluminum Nitride
AFM	Atomic force microscopy
Al ₂ O ₃	Sapphire
Ar	Argon
AlAs	Aluminum arsenide
Al	Aluminum
AMREC	Advanced Materials Research Centre
CL	Cathodoluminescence
CCl ₄	Carbon tetrachloride
CAIBE	Chemically assisted ion beam etching
C ₂ H ₅ OH	Ethanol
Cu	Copper
CCD	Charged couple device
CMOS	Complementary metal-oxide-semiconductor
C	Carbon
c-GaN	Cubic gallium nitride
DMF	Dimethylformamide
DMHy	Dimethylhydrazine
DBE	Exciton bound at a neutral donor
DAP	Donor acceptor pair
DI	Deionized
<i>e</i> A	Free electron to acceptor
e-beam	Electron beam

FE-SEM	Field emission scanning electron microscopy
fcc	Face-centered cubic
FWHM	Full-width half maximum
GaN	Gallium nitride
GaAs	Gallium arsenide
Ga	Gallium
H ₂ SO ₄	Sulphuric acid
HEMTs	High electron mobility transistors
HFETs	High field-effect transistors
hcp	Hexagonal closed-pack
HVPE	Hydride vapour phase epitaxy
HF	Hydrofluoric acid
HCl	Hydrochloric acid
H ₂ O	Water
H ₂ O ₂	Hydrogen peroxide
H ₃ PO ₄	Phosphoric acid
HeCd	Helium cadmium
H	Hydrogen
h-GaN	Hexagonal gallium nitride
ICP-RIE	Inductively-coupled plasma reactive ion etching
LEDs	Light emitting diodes
LDs	Laser diodes
MOSFETs	Metal-oxide-semiconductor field effect transistors
MBE	Molecular beam epitaxy
MOCVD	Metal organic chemical vapour deposition

Mo	Molybdenum
Mg	Magnesium
MOVPE	Metal organic vapour phase epitaxy
NH ₃	Ammonia
N	Nitrogen
Nb	Neobium
NBE	Near-band edge
NOR Lab	Nano Optoelectronics Research Laboratory
NaOH	Sodium hydroxide
O	Oxygen
PL	Photoluminescence
Pt	Platinum
PMT	Photomultiplier tube
p-Si	Porous silicon
RF	Radio frequency
RHEED	Reflection high-energy electron diffraction
RIE	Reactive ion etching
RBGE	Radical-beam gettering epitaxy
RMS	Root mean square
SSL	Solid state lighting
Si	Silicon
SiC	Silicon carbide
SLs	Superlattices
sccm	Standard cubic per centimetre
TiN	Titanium nitride

Ta	Tantalum
TD	Threading dislocation
UV	Ultraviolet
V_{Ga}	Gallium vacancy
$V_{\text{Ga}}\text{O}_{\text{N}}$	Gallium vacancy-oxygen complex
W	Tungsten
XRD	X-ray diffraction
XRC	X-ray rocking curve
Xe	Xenon
XPS	X-ray photoelectron spectroscopy

PENUMBUHAN LAPISAN GaN KE ATAS SUBSTRAT GaAs (100) MELALUI KAEDAH PERCIKAN FREKUENSI RADIO DAN PENYEJAT ALUR ELEKTRON

ABSTRAK

Kajian ini menunjukkan penumbuhan lapisan gallium nitrida (GaN) ke atas substrat gallium arsenida (GaAs) berliang melalui kaedah percikan frekuensi radio dan penyejat alur elektron. Sebagai perbandingan, penumbuhan secara terus ke atas substrat GaAs dan lapisan penampan nitrida seperti aluminium nitrida (AlN) dan titanium nitrida (TiN). Pada peringkat pertama kajian ini, parameter yang sesuai untuk menghasilkan GaAs berliang yang berkualiti dengan ketumpatan dan taburan yang seragam telah diperolehi. Didapati bahawa keseragaman dan ketumpatan liang yang tinggi boleh dicapai dengan campuran larutan dimetilformamida (DMF) dan asid sulfurik (H_2SO_4) dengan kepekatan DMF 75% selama 10 minit, pada ketumpatan arus 250 mA/cm^2 . Pada peringkat seterusnya, lapisan GaN ditumbuhkan secara berasingan ke atas permukaan yang berbeza melalui percikan frekuensi radio dan penyejat alur elektron. Bukti pengikatan Ga-N di dalam lapisan GaN diperhatikan melalui pengukuran spektroskopi fotoelektron sinar-x (XPS). Secara keseluruhan, penumbuhan lapisan GaN melalui percikan frekuensi radio mempamerkan permukaan yang rata berbanding dengan penumbuhan melalui penyejat alur elektron, tanpa mengira permukaannya. Walau bagaimanapun, pengukuran yang berkaitan dengan sifat-sifat struktur dan optik GaN mendedahkan bahawa semua lapisan GaN telah dibentuk dalam struktur amorfus. Untuk menangani isu ini, rawatan pasca-penyepuhlindapan pada suhu 980°C dalam persekitaran ammonia (NH_3) telah dilakukan selama 10 minit. Didapati bahawa sampel yang telah disepuh lindap mempamerkan struktur polihabluran. Permukaan sampel yang

telah disepuh lindap didapati kasar berbanding sampel GaN yang belum disepuh lindap disebabkan oleh pembentukan butiran-butiran berfaset dengan simetri yang berbeza. Proses penyepuhlindapan terhadap lapisan GaN yang ditumbuhkan melalui penyejat alur elektron ke atas substrat GaAs berliang dengan 75% kepekatan DMF menunjukkan peningkatan yang terbaik dalam sifat-sifat morfologi, struktur dan optik. Dalam eksperimen lain, struktur GaN berliang difabrikasi di atas lapisan GaN yang telah ditumbuhi melalui percikan radio frekuensi selama 3 minit dan 5 minit, masing-masing tanpa dan dengan menggunakan lapisan penampan AlN. Pengukuran mikroskop electron pengimbas pancaran medan (FE-SEM) dan mikroskop daya atom (AFM) menunjukkan bahawa struktur GaN berliang tanpa lapisan penampan AlN yang telah dipunar selama 3 minit mempamerkan liang keseragaman dan ketumpatan yang lebih baik berbanding yang lain, walaupun mempunyai permukaan yang kasar.

GROWTH OF GaN FILMS ON GaAs (100) SUBSTRATES BY RF-SPUTTERING AND E-BEAM EVAPORATION TECHNIQUES

ABSTRACT

This work studies the structure, morphology and optical properties of GaN layer grown on porous GaAs/GaAs substrate by radio frequency (RF) sputtering and electron beam (e-beam) evaporation. For comparison, the GaN layer was also grown directly on GaAs substrate and nitride based buffer layers, i.e. aluminum nitride (AlN) and titanium nitride (TiN). In the first part of this work, the best parameters used to obtain good quality porous GaAs on GaAs substrate with uniform distribution and density were determined. It was found that uniform distribution and high density of pores can be fabricated with a mixed solution of dimethylformamide (DMF) and sulphuric acid (H₂SO₄) with 75% DMF concentration for 10 minutes, at a current density of 250 mA/cm². In the next stage, the GaN layer was grown separately on different surfaces using RF-sputtering and e-beam evaporation. The evidence of Ga-N bondings inside the GaN layer was observed by XPS measurement. Overall, the GaN layers grown by RF-sputtering exhibited smoother surface as compared to one grown by e-beam evaporation, regardless of the surface growth. However, the measurement related to the structural and optical properties of GaN revealed that all GaN layers were amorphous in structure. To address this issue, post-annealing treatment at 980°C for 10 minutes in ammonia (NH₃) ambient was done on the samples. It was found that the annealed GaN samples were in polycrystalline structure. The rougher surface of the annealed GaN samples were rougher than the non-annealed GaN layers due to the formation of faceted grains with different symmetry. The annealing of the e-beam evaporated GaN layer on the porous GaAs/GaAs substrate with 75% DMF concentration showed the best

improvement in morphological, structural and optical properties. In another experiment, porous GaN was fabricated on the RF-sputtered GaN layer for 3 minutes and 5 minutes, respectively, with and without the insertion of AlN buffer layer. Field emission scanning electron microscopy (FE-SEM) and atomic force microscopy (AFM) measurements showed that the 3 minutes-etched porous GaN/GaN without the AlN buffer layer exhibited more uniform pore distribution and higher pore density compared to its counterparts, despite of the large surface roughness.

CHAPTER 1

INTRODUCTION OF GaN SEMICONDUCTOR

Energy consumption, especially in electricity sector in Malaysia has been progressively developed due to demand in improving human lifestyle. In recent years, Malaysia has spent about 112 billion kWh/per year for electricity alone [1]. One of the most common cause that contributed to the high electricity consumption is lighting. Introduction of solid-state lighting (SSL) technology like light emitting diodes (LEDs) has potential to reduce the energy usage. In comparison to conventional lighting sources, LEDs offers less power, consumption and can operate for longer hours [2].

Gallium nitride (GaN) material has received much attention from many researchers since the last few decades due to its unique characteristics compared to the other materials. This is due to its wide band gap, which is ~3.4 eV that allows it to operate at high temperature, high frequency and high power [3]. Such characteristic is advantageous for electronics and optoelectronics devices such as high-electron mobility transistors (HEMTs) [4, 5], high field-effect transistors (HFETs) [6, 7], metal-oxide-semiconductor field-effect transistors (MOSFETs) [8, 9], laser diodes (LDs) [10, 11], LEDs [12, 13] and others. With current rapid advancement in current technology today, GaN based power devices could be developed and this includes power supply and radio-frequency (RF) based devices.

Nonetheless, there are issues that ‘pull-back’ the development of GaN based devices to be adopted in wide range of applications. For example, limited availability of GaN substrate in the world market causes slow progress in the GaN based

technology. Alternatively, GaN is grown on foreign substrate such as sapphire (Al_2O_3), silicon (Si) and gallium arsenide (GaAs). Even though Si becomes the most preferable substrate for the GaN growth as it is available in larger size and cheap, GaAs could be a better substrate for growing GaN. This is because GaAs is a direct band gap material and it can promote better current injection to GaN based devices as high electron mobility and saturated electron velocity are possible compared to Si substrate [14, 15]. Growing GaN layer directly on GaAs substrate is considered challenging due to large lattice mismatch between both materials, which commonly results in high defects density inside the grown GaN layer [16].

Furthermore, the insertion of a buffer layer between GaN layer and GaAs substrate is a typical way to reduce defects density and cracks, as the impacts from the lattice mismatch. The problems are reduced, but the quality of the GaN layer still far from perfection. On the other hand, the introduction of porous GaAs layer on GaAs substrate could give a better solution to the problem. The surface of porous GaAs could be able to 'sink' the defects specifically threading dislocations while releasing strain in the GaN layer. Therefore, the fabrication of GaN could be simplified without the use of buffer layer.

While most works are focusing on growing GaN layer using popular techniques like molecular beam epitaxy (MBE) and metal organic chemical vapour deposition (MOCVD), it is possible to grow GaN layer at an acceptable level of quality in a much simple and low-cost manner using RF-sputtering and electron beam (e-beam) evaporation. Both techniques are inexpensive and simple with easy operation to grow semiconductor materials, especially GaN.

The main scope of study in this work includes; (1) growth of GaN layer using RF-sputtering and e-beam evaporation, (2) fabrication of porous GaAs using photo-electrochemical etching and (3) annealing treatment to improve the quality of GaN layer using 3-zone furnace under ammonia (NH₃) ambient. The aim of this work is to investigate the effect of GaN layer grown on porous GaAs in order to obtain a good quality of GaN layer. Thus, the main objectives to fulfill this aim are;

- 1) to obtain good quality porous GaAs on GaAs substrate with uniform distribution and density.
- 2) to achieve good quality of grown GaN layer directly on porous GaAs/GaAs substrate using RF-sputtering and e-beam evaporation.
- 3) to improve the properties of GaN layer by annealing process.

In this work, the GaN layer was also grown directly on GaAs substrate and nitride based buffer layers, i.e. aluminum nitride (AlN) and titanium nitride (TiN) for comparison.

The content of this thesis is organized as follows:

Chapter 2 describes the basic properties of GaN material in both hexagonal and cubic structures. Details of the research progress of GaN grown on foreign substrates are given. Furthermore, the progress on the fabrication of porous GaAs on GaAs substrate, GaN grown on porous GaAs/GaAs substrate and annealing treatment of GaN layer is also reviewed.

Chapter 3 encompasses preparation and experimental procedures covering the fabrication of porous GaAs, growth process of GaN layer, post-annealing of the GaN sample and the characterization measurements used in this work. Issues that have

been encountered while doing the fabrications and characterizations also will be discussed and the solutions are proposed.

Chapter 4 focuses on the fabrication of porous GaAs (100) substrate using photo-electrochemical etching technique with different conditions. The results of the porous GaAs are presented, specifically on the morphological aspect through field-emission scanning electron microscopy (FE-SEM) measurement. The best etching parameters that produce high uniformity and pores density of porous GaAs will be proposed.

Chapter 5 emphasizes on the properties of GaN layer grown on porous GaAs substrate, together with the GaN grown on GaAs substrate and nitride based buffer layer (AlN and TiN) using RF-sputtering and e-beam evaporation. The effect of the properties of GaN layer grown on different surface will be discussed from the morphological aspect. In addition to that, the fabrication of porous GaN/GaN layer grown on GaAs substrate with and without the insertion of AlN buffer layer at different etching time will be demonstrated. The morphological, structural and optical properties of the porous GaN/GaN layer will be presented and the best porous GaN will be proposed.

Chapter 6 reports the effect of thermal annealing treatment using different temperature on the RF-sputtering and e-beam evaporation grown GaN samples, with different annealing temperatures. The annealed GaN samples will be characterized by investigating their morphological, structural and the optical properties. The best annealing temperature will be proposed. Next, the annealing treatment of the grown GaN samples on different surface will be conducted. The best annealed GaN sample will be suggested through morphological, structural and optical properties.

Chapter 7 concludes the findings of this work. Few suggestions of the future works to improve the quality of this research will be provided.

CHAPTER 2

BASIC PROPERTIES AND LITERATURE REVIEW OF GaN

This chapter begins with a short description on the atomic arrangement of GaN material. It is well-accepted that this understanding is important to strategize way to improve GaN layers. The basic properties of hexagonal GaN and cubic GaN also will be presented. This is followed by a review on published works with regards to current issues and progress on the growth of GaN, including the use of nitride based buffer layer and porous layer in the technology of GaN growth. Subsequently, survey from literature on the improvement of GaN material by thermal annealing treatment will be provided towards the end of this chapter.

2.1: Basic introduction to GaN material

Gallium nitride (GaN) is a promising semiconductor material with wide band gap of ~3.4 eV that has big potential in high power and high frequency based devices such as light emitting diodes (LEDs), laser diodes (LDs), high-electron-mobility transistors (HEMTs) and others. So far, epitaxial growth of the GaN is conducted using foreign substrates, i.e. silicon (Si), gallium arsenide (GaAs), sapphire (Al_2O_3) and silicon carbide (SiC). This is due to the difficulty in producing bulk GaN substrate at low-cost.

Generally, GaN structure is formed in two phases; (1) hexagonal (wurtzite) structure and (2) cubic (zinc-blende) structure. Hexagonal GaN structure is thermodynamically stable phase, whereas cubic GaN structure is metastable structure in nature. Figure 2.1 shows the atomic arrangement of both hexagonal and cubic structure in GaN materials. The atoms in hexagonal structure are arranged in

hexagonal close-packed (hcp) unit, which consists of two lattice constants denoted as a and c . On the other hand, the atoms in cubic structure are formed in cubic unit cells (face-centered cubic (fcc)), which has similar distance with high crystal symmetry as its lattice constants are equal in three perpendicular directions (all directions denoted as a). Nevertheless, the stacking sequence of the hexagonal and cubic structure is different. The stacking sequence in hexagonal structure is ABABAB while the stacking sequence in cubic structure is ABCABC, as been illustrated in figure 2.2.

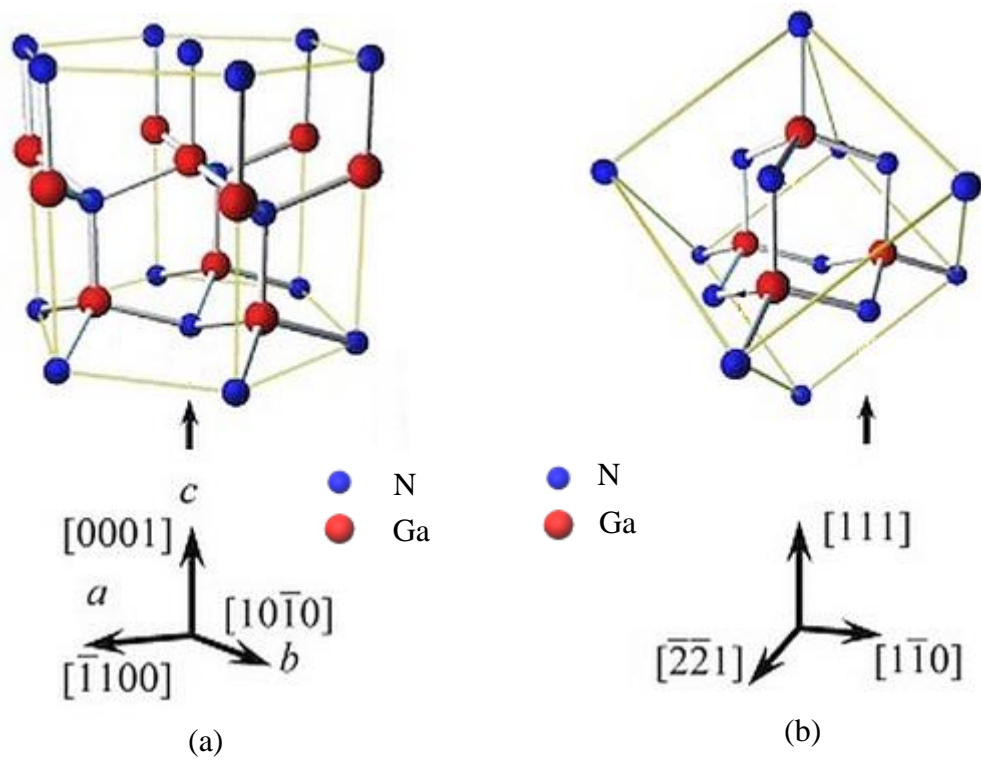


Figure 2.1: Atomic arrangement in (a) hexagonal (wurtzite) and (b) cubic (zinc-blende) GaN material. The images were taken and modified from [17].

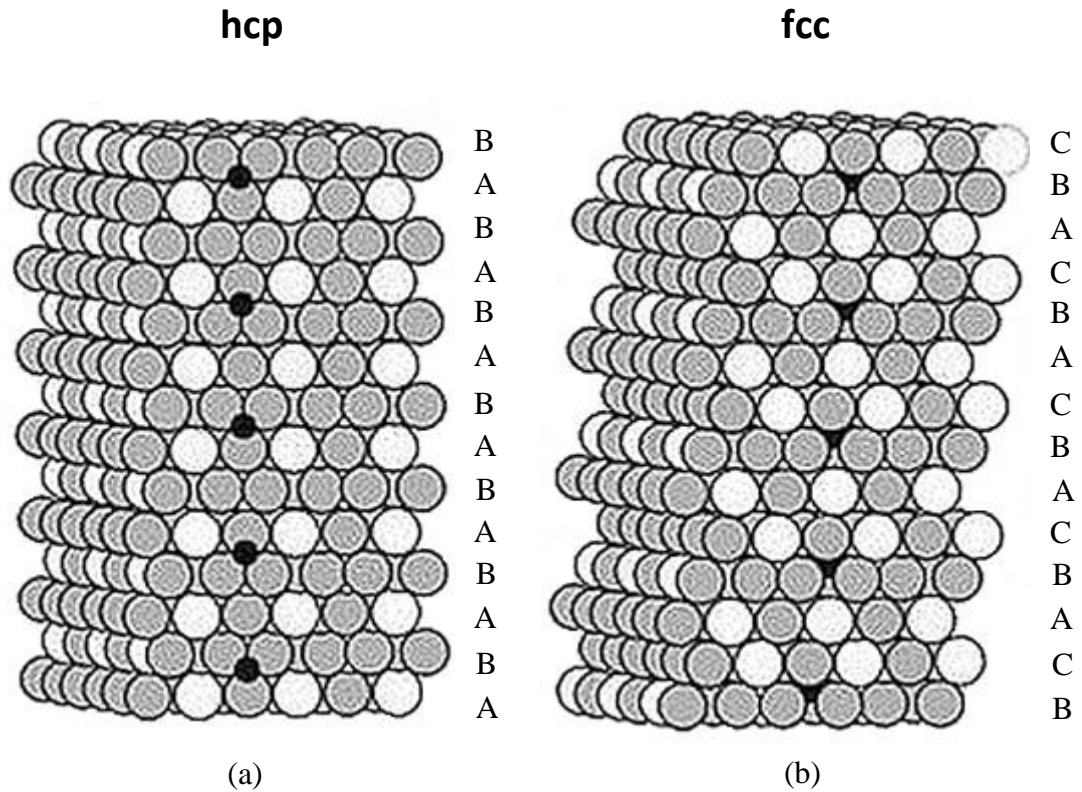


Figure 2.2: Stacking sequence of atoms in (a) hexagonal and (b) cubic structure. The images were taken and modified from [18].

Table 2.1 shows the basic properties of the GaN material in both hexagonal and cubic phase structures. These values are commonly used in many works. In terms of stability, hexagonal GaN is more stable rather than cubic GaN. Hence, the growth of hexagonal GaN and cubic GaN should be done in specific conditions. In general, cubic GaN growth is very tricky, thus requires proper technique to obtain high purity cubic GaN due to its metastable structure in nature. The value of the energy band gap of cubic GaN is always smaller than the hexagonal GaN. Here, the different value of the lattice constant in hexagonal and cubic GaN structure is due to the difference in atomic arrangements in both structures. The presented values of the theoretically lattice constant for hexagonal and cubic GaN are shown in the table. The presence of strain inside the material can vary the value of the lattice constants determined from the theoretical calculation [19]. Note that the material will

experience compressive stress when its lattice constant values is smaller with respect to the theoretical values and vice-versa if it experiences tensile stress. To the best of my findings, there are very few reported data for cubic GaN, like electron affinities and thermal expansion coefficient as the growth of cubic nitrides are challenging.

Table 2.1: Basic properties of hexagonal and cubic GaN structure.

Properties	Hexagonal GaN	Cubic GaN
Structure	Wurtzite	Zinc-blende
Stability	Stable	Metastable
Energy gap, E_g (T = 0K) (eV)	3.40 [20]	3.30 [21]
Energy gap, E_g (T = 300K) (eV)	3.46 [22]	3.23 [21]
Lattice constant, (\AA) (theoretical values)	$a_0 = 3.189$ $c_0 = 5.185$	4.500
Thermal expansion coefficient (K^{-1}) (T ~300K)	Along $a_0 = 3.7 \times 10^{-6}$ [23] Along $c_0 = 2.8 \times 10^{-6}$ [23]	-
Electron affinity, χ (eV)	4.1 [24]	-
Effective electron mass, m_e	0.22 m_0 [25]	0.15 m_0 [26]

2.2: Choice of substrate for GaN growth

Homoepitaxial growth of GaN layer on GaN substrate is less demonstrated due to limited availability of bulk GaN substrate. Therefore, GaN layer is always grown using foreign substrate (heteroepitaxy). Nevertheless, the choice of substrate is an essential factor for successful growth and good layer properties of GaN. So far, GaN films have been grown on several substrates, for example; sapphire (Al_2O_3) [27, 28], silicon (Si) [29, 30] and gallium arsenide (GaAs) [31, 32]. Among them, GaAs substrate is more preferable because it has high electron mobility and saturated electron velocity, which can promote better current injection to the GaN based devices.

2.2.1: Comparison between GaAs substrate and other substrate for GaN growth

In many reports, the growth of GaN on sapphire certainly lead to good structural quality, even though the lattice mismatch between GaN and sapphire is relatively high (~14%) [33]. Normally, the hexagonal structure of sapphire substrate will result in the growth of hexagonal phase GaN. Despite of this, the insulating and hardness characters of sapphire could be a major problem for GaN based device fabrication. According to Hong et al. [34], the insulating character of sapphire substrate has impeded the progress towards large scale integration of GaN based devices, especially in vertical transport devices like LEDs. Furthermore, it is found that the sapphire substrate is hard to be etched and as a result, it is difficult to fabricate the GaN based devices in large scale [35]. Group of Tsuchiya et al. [36] have found that the laser diodes (LDs) fabricated on sapphire facing severe problems such as high series resistance or degradation of the laser performance. Meanwhile, Yang et al. [37] proposed that the fabrication of laser cavities for GaN-based heterostructure on sapphire has problems of the incompatible cleavage planes of GaN and substrate. With rapid advancements of fabrication technology nowadays, the lift-off process of the sapphire from the GaN layer can be done, however, it is complicated and not cost-effective process. Unlike sapphire, GaAs can easily be cleaved and etched, which is good for device fabrication [38]. Moreover, the etching process of the GaAs from the GaN layer is simple and very cost-effective. It is easily etched by immersing it into aqua regia, which does not ‘wipe out’ the GaN layer away [39]. In addition, GaAs substrate is considered to be low cost compared to sapphire substrate.

On the other hand, Si has been widely used as a substrate for GaN growth. It is because Si is available in large size and is more cost-effective compared to other

material like GaAs. However, Si has an indirect band gap, so that it is not suitable for emitting light. Unlike Si, GaAs has a direct band gap, which can be used to absorb and emit light efficiently. Next, the electron mobility and saturated electron velocity of Si is found to be $\leq 1400 \text{ cm}^2/\text{Vs}$ and $1.0 \times 10^7 \text{ cm/s}$, respectively, while, for GaAs it is found to be $\leq 8500 \text{ cm}^2/\text{Vs}$ and $1.2 \times 10^7 \text{ cm/s}$, respectively. Since GaAs has higher electron mobility and saturated electron velocity than Si, it will promote a better current injection to the GaN based devices. Later on, the GaN layer will exhibit severe wetting problems when it is grown directly on Si substrate, which results in poor quality and morphology of GaN layer [40, 41]. Nonetheless, GaAs has a thermal expansion coefficient closer to GaN than other substrates, thus it is unlikely to cause cracks due to thermal stress [42]. Therefore, it can be concluded that GaAs could be a good substrate for growing GaN and manufacturing GaN based devices.

2.2.2: GaAs surface orientation: GaAs (111) versus GaAs (100)

Up to now, the GaN layer was grown onto GaAs (111) substrate orientation using molecular beam epitaxy (MBE) [43, 44], metal organic chemical vapour deposition (MOCVD) [45] and hydride vapour phase epitaxy (HVPE) [42, 46]. Nonetheless, there are some problems related to the growth of GaN on GaAs (111) substrate. Note that GaAs (100) has more potentials than GaAs (111) as it has a higher geometrical symmetry of the Ga and N atoms, which is good for the development of light emitting diodes (LEDs) and laser diodes (LDs), as mentioned before. Unlike GaAs (111) substrate, the cleaving in [100] direction for GaAs (100) substrate is easier without detrimental the wafer as compared to GaAs (111) substrate orientation. It is difficult to cleave GaAs along {111} planes. It is because

these planes consist of alternate layers of group III and group V atoms, which results in strong electrostatic attraction between them [47]. Meanwhile, the cleavage of GaAs (100) is most preferred along on the perpendicular {110} planes, which can eliminate such electrostatic attraction between group III and group V since they contain an equal gallium (Ga) and arsenic (As) atoms [47].

2.3: Progress of GaN growth on foreign substrate

In many works, the growth of GaN layers on foreign substrate has widely been demonstrated using advanced and low-cost techniques. For the advanced technique like MBE and MOCVD, most of the published works demonstrate the growth of single crystalline GaN layer [48-50]. Instead of growing single crystal structure, there is still few reported works on the growth of polycrystalline GaN using either MBE or MOCVD [51-53]. Meanwhile, for the low-cost technique like sputtering and e-beam evaporation, most of the reported works demonstrate the growth of polycrystalline GaN structure [54-56]. Even though single crystal GaN structure shows better crystalline quality compared to polycrystal GaN structure, but having GaN in polycrystalline structure could exhibits some advantages especially in the optical properties [57-59]. Next, the survey of some reported works on the growth of GaN layers using both advanced and low-cost techniques will be given below.

i) Growth of GaN by MBE

The growth temperature and the gas flow rate play an important role in obtaining high quality GaN layer with preferred growth orientation. In 1998, group of Murata et al. [57] has successfully grown polycrystalline GaN layer on silica substrate. They have found that the polycrystalline GaN growth with *c*-oriented plane at 750°C and the nitrogen (N₂) gas flow rate of 30 sccm. Interestingly, the polycrystalline GaN layer showed five time stronger photoluminescence (PL) intensity than the single crystalline GaN. The full width half maximum (FWHM) of low-temperature PL measurement for polycrystalline GaN layer and single crystalline GaN on sapphire were found to be 62.7 meV and 85.9 meV, respectively. However, no detailed explanation on this behaviour was given. It is suggested that the rough surface of the polycrystalline structure could reduce the total internal reflection, so that more light will be emitted. A year later, Asahi et al. [58] also have investigated the growth of polycrystalline GaN layer on silica substrate. At this time, they have used low N₂ gas flow rate (~1.0 - 1.5 sccm) with the gallium (Ga) flux of 1-3×10⁷ Torr. It is found that the PL intensity of the polycrystalline is higher than the one of single crystalline GaN grown on sapphire. However, the FWHM of the sample was found to be (400 meV), which is wider by a factor of 5-8 than the GaN on sapphire. Later, Hiroki et al. [59] studied of polycrystalline GaN grown on silica substrate by varying the growth temperature from 700°C - 800°C while fixing the N₂ gas flow rate and Ga flux ratio same with previous survey by Hiroki and his teams. By using various temperatures, the optical properties of polycrystalline GaN layer was much improved. It was found the FWHM of low-temperature PL measurement was found to be around 32 meV under optimized growth condition. According to Tambo et al. [60], the growth temperature played an important factor to

get high quality polycrystalline GaN layer rather than Ga/N₂ flux ratio. However, they did not mention the best growth temperature in their works. In addition to that, Choi et al. [61] had successfully demonstrated the growth of nearly single crystalline GaN on glass substrate at high temperature of ~1040°C. It was found that the FWHM of room-temperature cathodoluminescence (CL) of their sample (158 meV) to be almost similar with the single crystalline GaN grown on sapphire [62], revealing high optical quality.

On the other hand, the grains size also plays an important factor to get high quality GaN with preferred growth orientation. Hiroki et al. [59] grown the GaN layer with the grains size around 100-200 nm. In the early stage of growth, the reflection high-energy electron diffraction (RHEED) patterns showed weak ring patterns revealing polycrystalline layer without orientation. Based on the experience in growing GaN layer, it was found that the grain size will increase with the increasing thickness of the GaN layer. Hence, it is believed that the bigger grain size will improved the quality of the GaN layer. According to Nouet et al. [63], grain size is an important factor to control PL emission. They have found that the bigger grain size showed narrower FWHM of PL measurement than the one with small grain size.

Group of Araki et al. [51] had investigated the effect of nitridation on the quality of the overgrown GaN layer. After the GaN grown on silica glass substrate at 700°C, the nitridation was performed at 700°C for 1 hour. Based on the RHEED patterns, it is found that the GaN layer without nitridation shows poor *c*-axis oriented polycrystalline structure. Meanwhile, the RHEED patterns showed spot-streak patterns, indicating that the highly oriented polycrystalline structure was observed. It is suggested that the nitridation process also improves the crystalline quality of the GaN layer. Such improvement clearly confirmed by XRD rocking curve (RC)

measurement, which revealed the FWHM of the nitridized GaN found to be less than 1° . On the other hand, Maksimov et al. [64] revealed that the nitridation performed at low temperature (400°C) exhibits single crystalline GaN structure. It is concluded that the nitridation process at certain temperature affected the preferred growth orientation of GaN layer.

Besides that, the choice of the substrate was one of the criteria to achieve preferential growth of GaN layer. Group of Yamada et al. [52] had investigated the growth of GaN layer on quartz and several metal substrates, which are tungsten (W), molybdenum (Mo), tantalum (Ta) and niobium (Nb). It is shown that the GaN/W, GaN/Mo and GaN/quartz preferred to grow towards GaN (0002) orientation. In contrast, GaN/Ta and GaN/Nb showed preferential GaN ($10\bar{1}1$) orientation. In the meantime, Hasegawa et al. [53] studied the growth of polycrystalline GaN layer on MO sheets and Si (001) substrate. Interestingly, the polycrystalline GaN grown on MO sheets showed good field emission characteristics due to the grain structures and low electron affinity as compared to the one grown on Si substrate.

ii) Growth of GaN by MOCVD

Meanwhile, Miyoshi et al. [65] had investigated the GaN grown on GaAs (100) using different types of nitrogen (N) precursors which are dimethylhydrazine (DMHy) and ammonia (NH_3). It is found that the optimum parameter to get high quality GaN layer for DMHy was found to be 650°C at V/III ratio of 160 while for NH_3 was found to be 600°C at V/III ratio of 4900. The use of small amount of DMHy would be enough to obtain high quality of GaN layer. According to Pérez-Solórzano et al. [66], the use of NH_3 at low temperature is inefficient since it requires higher V/III ratios (> 10000) to obtain a good optical quality. As a result,

the waste materials that produced during the growth was drastically increased. Group of Zheng et al. [67] had grown the GaN layer on GaAs (001) with the NH_3 flow rate of $17800 \mu\text{mol}/\text{min}$ by MOCVD. On the other hand, there are some disadvantages of using DMHy as a precursor. First, it decomposes at lower temperature and it is not suitable for GaN or other materials growth under growth temperature above 1000°C [68]. Second, relatively high levels of oxygen and carbon ($>10^{19} \text{ cm}^{-3}$) were found, both are associated with the use of DMHy as precursor. Moreover, Kobayashi et al. [69] suggested that DMHy precursor cannot be used for the growth of GaN at atmospheric pressure. However, such suggestion can be argued since the growth of GaN on GaAs (001) at atmospheric pressure using DMHy had been demonstrated by Tachibana et al. [70].

Besides that, the growth temperature of GaN grown by MOCVD was one of the important criteria to achieve high quality GaN layer. It is worth noting that the growth temperature applied might not similar when the GaN layer grown on different substrate. According to Miyoshi et al. [65], there is no growth of GaN layer on GaAs substrate at lower temperature (500°C). Interestingly, six years later, Zheng et al. [67] successfully grew GaN layer on GaAs (001) at 520°C by introducing CCl_4 as additive precursors, which is the lowest temperature reported for the GaN growth by MOCVD. Meanwhile, for the GaN grown on sapphire substrate, the optimize growth temperature used to obtain high quality GaN layer was found to be in the range of $1030^\circ\text{C} - 1080^\circ\text{C}$ [71-73]. Later, the optimize growth temperature in order to get better quality of GaN grown on silicon substrate was found to be in the range of $1040^\circ\text{C} - 1060^\circ\text{C}$ [74-76].

On the other hand, the growth pressure applied also one of the important parameter that can affect the quality of GaN layer. According to Guarneros et al.

[49], the single crystalline GaN grown on sapphire substrate can be achieved when the low-pressure MOCVD growth process (100 mbar) was applied. At the same time, Cervantes et al. [77] proposed that the optimum pressure for the GaN grown on sapphire substrate was at 76 Torr (~101 mbar), which exhibits superior structural and optical properties. They also claimed that the GaN layer grown at higher pressure showed hexagonal pits and surface spiral that strongly affected morphology, structural and optical properties of GaN.

iii) Growth of GaN using RF-sputtering and e-beam evaporation

With rapid advancements in fabrication technology nowadays, it is possible to grow GaN layer at an acceptable level in quality in a much simple and low-cost manner. RF-sputtering and electron beam (e-beam) evaporation techniques are inexpensive techniques with easy operation that may suitable to grow semiconductor materials, especially GaN.

Group of Preschilla et al. [78] had demonstrated the growth of GaN layer using reactive sputtering with different temperature. It was found that at low temperature of 400°C - 550°C, the GaN layer exhibits polycrystalline phase structure. Meanwhile, at higher growth temperature of 600°C, single crystal of hexagonal GaN (0002) orientation was found to be dominant. This finding suggested that the growth orientation is dependent on the growth temperature. Later, Knox-Davies et al. [79] had grown GaN layer on Si (001) and fused quartz substrate with variation of temperature starting from room temperature to 450°C using sputtering technique. They found that the most crystalline layer was grown at mid range temperature, however, no specific temperature value has been given. A year later, Yadav et al. [54] revealed that the growth temperature below 300°C showed the GaN layer

dominantly grown in amorphous phase structure. Meanwhile, the polycrystalline dominantly grown when the growth temperature is above 300°C. Through this survey, it is suggested that the growth temperature are needed to be applied while growing GaN layer in order to get better quality sample. However, the best growth temperature cannot be specified since the specifications of sputtering machine used by other works may be not the same.

It is worth highlighting that the gas flow ratio applied while growing the GaN also plays an important parameter to achieve high quality layer. Elkashef et al. [55] have investigated the effect of using different gas flow ratio on the structural aspects of the GaN layer. It was found that with the presence only 10% N₂ in argon (Ar) gas, the broad peak of GaN (10 $\bar{1}$ 0) and (11 $\bar{2}$ 0) orientations were observed, revealing the layer mostly grown in amorphous structure. When 100% N₂ was used, polycrystalline GaN (10 $\bar{1}$ 0), (0002) and (10 $\bar{1}$ 1) orientations were observed. Later on, Song et al. [80] also found that the GaN layer grown with 100% N₂ gas flow exhibits <0001> preferred orientation polycrystalline GaN. The sputtering GaN layer with N₂ gas enhances the nitrogen incorporation and prevents the degradation of crystal structure, resulting the GaN layer to be stoichiometric [81]. On the other hand, Zou et al. [82] have revealed that the XRD peak intensity of GaN (0002) orientation reaches a maximum value when Ar to N₂ ratio was 50%, which is contrast with the previous surveys.

Next, the pressure applied during the growth process is another factor to obtain better quality of GaN layer. According to Leite et al. [83], they found that the GaN layer grown at higher pressure ($\sim 10^{-2}$ mbar) was amorphous structure. Hence, group of Miyazaki [84] have shown that a strong peak related to GaN (0002) was

observed at lower pressure ($\sim 10^{-3}$ mbar), indicating that the layer grown at lower pressure has a high preferred orientation towards c-plane. In addition, similar evidence was also reported by Li et al. [85]. Based on these findings, the interest in the growth of GaN using sputtering will be further enhanced.

Up to date, there is only one reported work related to the growth of GaN layer using e-beam evaporation. This technique is not popular among the grower might be due to the poor morphological quality of the films. Prior to this, e-beam evaporation mostly been used to deposit metal contact in device fabrication. E-beam evaporation is another low-cost technique that suitable to grow the epitaxial layer like GaN compared to the advanced techniques like MBE and MOCVD. The mechanism process of the e-beam evaporation is not the same as sputtering technique. Detailed explanation about the mechanism process will be given in Chapter 3. Note that the growth of GaN layer using e-beam evaporation has only been demonstrated by Chaudhari et al. [56]. Their works were focused on the growth of GaN on Si (100) substrate using different growth temperatures. The GaN layer grown at temperature below 300°C showed amorphous structure. Meanwhile, the GaN growth at 600°C showed polycrystalline structure.

Overall, the quality of the GaN layers grown by sputtering and e-beam evaporation is still far from expectation as compared to the advanced techniques like MBE and MOCVD. Junaid et al. [86] had demonstrated the dislocation density of GaN grown using sputtering was estimated to be as low as $\sim 10^9$ cm⁻², which is a magnitude higher than either MBE or MOCVD samples [27, 87]. In addition, the FWHM of the XRD rocking curve (RC) was found to be 1054 arcsec, which is comparable to the one single crystalline GaN grown on sapphire using advanced techniques [88, 89]. However, growing GaN directly on foreign substrate will result

in different lattice mismatch between GaN and substrate that causes the formation of strain and dislocation, which affected the quality of the GaN. By introducing buffer layer between the overgrown GaN layer and substrate, such problems will be minimized. Here, the motivation of use RF-sputtering and e-beam evaporation in this work is to simplify the growth technique while slash the cost production when it was compared to MBE and MOCVD. As a benefit, devices base on this are affordable to everyone.

2.4: Role of buffer layer on growth of GaN material

Growing GaN directly on GaAs substrate is considered challenging due to large lattice mismatch between both materials, which commonly results in high defects inside the grown GaN layer [16]. Figure 2.3 illustrates the formation of mismatch dislocation in GaN layer grown directly on GaAs substrate.

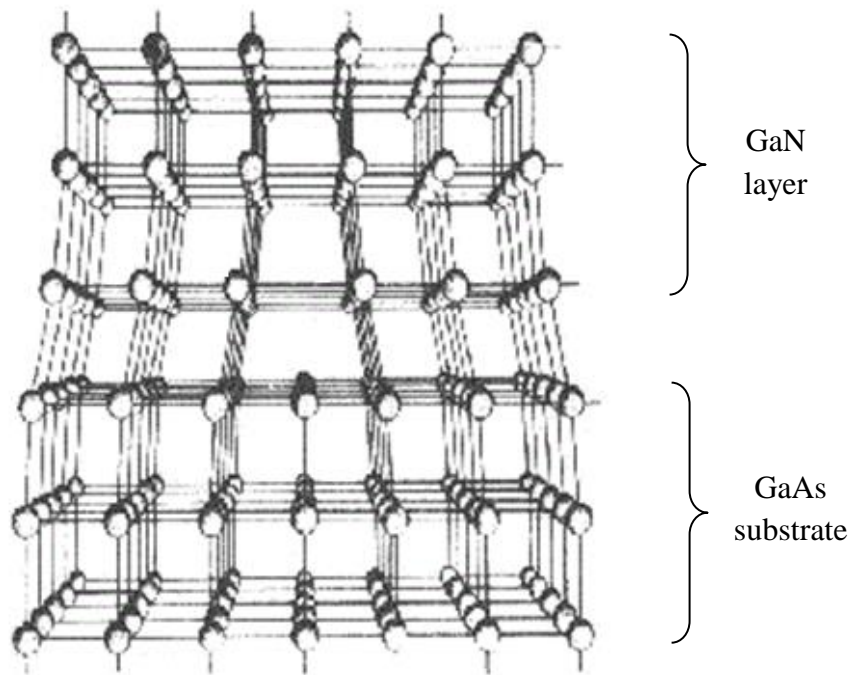


Figure 2.3: Formation of mismatch dislocation in GaN layer grown directly on GaAs substrate. The image has been taken and modified from [90].

Introduction of buffer layer as the intermediate layer between the GaN and GaAs substrate is possible to reduce the tensile stress and hinder the cracks formation in the GaN layer. Figure 2.4 illustrates the lattice arrangement in GaN layer without and with the insertion of buffer layer. It shows that the idea where the overgrown layer exhibits better structure when the buffer layer was inserted, which the impact from the lattice mismatch has been reduced.

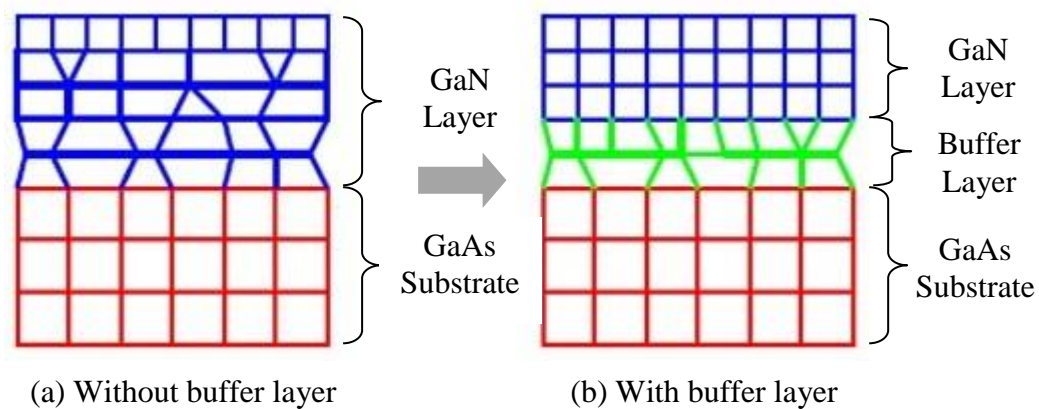


Figure 2.4: Schematic diagram to explain the idea of lattice arrangement in GaN layer grown on GaAs substrate (a) without and (b) with the insertion of buffer layer. The image is taken and modified from [91].

So far, several materials have been widely used as the buffer layer for GaN layer, for example aluminum nitride (AlN) [92], titanium nitride (TiN) [93, 94], GaN [71, 92, 95-97], AlN/GaN superlattices (SLs) [71, 98] and aluminum arsenide (AlAs) [99] and others. Review on the reported works on the use of various buffer layers for the growth of GaN layer are summarized in Table 2.2. AlN buffer layer has been widely used in the growth of GaN on Si substrate in order to reduce the impacts of the lattice mismatch ($\sim 2.5\%$) and thermal expansion coefficient between both materials [40, 100]. However, only few works on the growth of GaN layer on GaAs substrate with the introduction of AlN buffer layer have been reported. According to Li and his team [92], the insertion of AlN buffer layer between GaN and GaAs

substrate favoured the hexagonal GaN (0002) growth. They suggest the hexagonal AlN structure was energetically preferred on the surface of GaAs substrate when the AlN buffer layer was grown. It is known that the AlN is naturally acting as insulator and if the thicker layer were grown, it somehow affects the vertical transport properties in devices, for example light emitting diodes (LEDs).

On the other hand, TiN is the transition metal nitride that has good properties and makes it suitable to be used as buffer layer for GaN growth. It has small lattice mismatch (~6.2%) between GaN and TiN, conductive material, low electrical resistivity (~15-100 $\mu\Omega\text{cm}$), and a high melting point of 2950°C. The use of TiN as a buffer layer for GaN growth has been demonstrated in 2005 by Watanabe et al. [93]. It was followed by Ito et al. [94] four years later. They have managed to grow smooth GaN layer on TiN buffer layer. However, this study was conducted using sapphire substrate. Up to date, no reports to date have demonstrated the growth of GaN on GaAs substrate with the insertion of TiN buffer layer. It will be good if such structure can be investigated in order to diversify the use of TiN material for future applications.

Meanwhile, the use of GaN buffer layer has been widely reported in many published works. Such buffer layer is preferred to be used in the growth of GaN layer since the problems of the lattice mismatch is almost negligible. In 1991, Nakamura [97] has demonstrated the growth of GaN layer using GaN buffer layer on sapphire substrate. It was found that the GaN grown on GaN buffer layer exhibits flat and smooth surface. The same result was obtained by Li et al. [92], which the GaN layer grown on GaN buffer layer/GaAs (001) substrate exhibits smoother surface with the lateral growth. Nevertheless, Li et al. [71] were found that the GaN layer grown on GaN buffer layer/sapphire substrate appears opaque with high

density of hexagonal pits. Thus, they proposed the growth of mirror-like surface GaN layer on AlN/GaN superlattices (SLs) structure, which can improve the quality of GaN layer better than the one grown on GaN buffer layer. Meanwhile, the introduction of AlN/GaN SLs between the growth of GaN layer and Si substrate has improved the structural quality of GaN layer, but not successful in reducing crack density on the surface [98]. It seems that the use of SLs structure is complicated since the thickness and the amount of GaN/AlN period of each layer needs to be optimized.

On the other hand, the use of AlAs buffer layer has been demonstrated by Liu et al. [99]. They found that the use of AlAs buffer layer in the growth of GaN on GaAs substrate tends to promote the formation of hexagonal phase structure. It might be due to the lattice mismatch between GaN and AlAs since its lattice constant (5.6605 Å) near to GaAs lattice constant (5.6533 Å). The earlier published works on the growth of GaN, with the various uses of different buffer layers are summarized in Table 2.2.

It is worth highlighting that the use of buffer layer which can be considered as typical way to overcome the high lattice mismatch and propagation of the defects between GaN and the GaAs substrate. However, the introduction of the porous GaAs is potentially giving a new breath in solving such problems, where the introduction of the buffer layer is no longer needed. Moreover, the fabrication process of GaN could be simplified at low-cost level since the amount of waste material could be minimized. The reviewed works related to the fabrication of porous GaAs structure are given in the section below.

Table 2.2: Summary of the GaN grown on foreign substrate with different buffer layer.

Buffer layer	Advantage	Disadvantage	Reference
AlN	-Small lattice mismatch (2.5%)	-Insulator -Exhibits rougher surface -Preferred hexagonal growth	[92]
TiN	- Small lattice mismatch (6.2%)	- Never been applied on GaAs substrate	[92], [101], [102]
GaN	- Exhibits smoother surface - No lattice mismatch	- High density of hexagonal pits	[92], [97], [71]
AlN/GaN superlattices (SLs)	- Mirror-like surface - Improve GaN quality	- Complicated process - Cannot reduce crack density	[71], [98]
AlAs		- Preferred hexagonal growth - High lattice mismatch	[99]

2.5: Introduction of porous GaAs and its progress

Porous GaAs has been identified as a potential surface for promoting low threading dislocations and strain in the overgrown epitaxial layer [103]. However, producing porous GaAs in a well-defined structure with high pore distributions density is quite challenging. With rapid advancements in technology nowadays, many researchers have established the fabrication of the porous structure. Generally, porous structure can be obtained through two types of etching technique; (1) dry-etching and (2) wet-etching. There are several types of dry etching, which includes reactive ion etching (RIE) [104, 105], inductively-coupled plasma reactive ion etching (ICP-RIE) [106, 107], chemically assisted ion beam etching (CAIBE) [108,